

Magnetic field induced flop of cycloidal spin order in multiferroic TbMnO₃: The magnetic structure of the $P||a$ phase

N. Aliouane,^{1,2} K. Schmalzl,³ D. Senff,⁴ A. Maljuk,¹ K. Prokeš,¹ M. Braden,⁴ and D. N. Argyriou^{1,*}

¹Helmholtz-Zentrum Berlin für Materialien und Energy, Glienicker Str. 100, D-14109 Berlin, Germany

²Institute For Energy, P.O. Box 40, NO-2027 Kjeller, Norway

³Institut für Festkörperforschung, Forschungszentrum Jülich GmbH, JCNS at ILL, 38042 Grenoble Cedex 9, France

⁴II. Physikalisches Institut, Universität zu Köln, Zùlpicher Str. 77, D-50937 Köln, Germany

(Dated: September 14, 2021)

Using in-field single crystal neutron diffraction we have determined the magnetic structure of TbMnO₃ in the high field $P||a$ phase. We unambiguously establish that the ferroelectric polarization arises from a cycloidal Mn spins ordering, with spins rotating in the ab plane. Our results demonstrate directly that the flop of the ferroelectric polarization in TbMnO₃ with applied magnetic field is caused from the flop of the Mn cycloidal plane.

PACS numbers: 61.12.Ld, 61.10.-i, 75.30.Kz, 75.47.Lx, 75.80.+q

The antisymmetric Dzyaloshinski-Moriya (DM) interaction[1, 2] between two spins, S_i , S_{i+1} separated by $r_{i,i+1}$, provides for a natural coupling between magnetism and ferroelectricity with the spontaneous ferroelectric polarization given by $\mathbf{P}_s \sim \mathbf{r}_{i,i+1} \times (\mathbf{S}_i \times \mathbf{S}_{i+1})$ [3, 4, 5]. This mechanism generates ferroelectricity in a wide variety of magnets such as $RMnO_3$ perovskites with $R=\text{Gd, Dy, and Tb}$, [6, 7], spinel chromate CoCr_2O_4 , [8] spin-chain cuprate LiCu_2O_2 , [9] and hübnerite MnWO_4 [10, 11]. In the $RMnO_3$ manganites the DM interaction results in cycloidal order of Mn-spins giving a spontaneous ferroelectric polarization along the c -axis ($P||c$) (Fig. 1(a)). The application of magnetic field results in the flop of the polarization from the c - to the a -axis and highlights a novel control of one ferroic property by another [6]. It has been assumed that this change in the direction of the polarization reflects the flop of the Mn spin cycloid, implying that the antisymmetric DM interaction continues to be responsible for the polarization (Fig. 1(b)) [3, 12]. However, in this high field $P||a$ -phase, the commensurate magnetic wave vector for Mn is also compatible with other magneto-electric mechanisms such as exchange striction [13, 14, 15]. In this letter we present a determination of the magnetic structure of TbMnO₃ in a high magnetic field in the commensurate $P||a$ phase. We find that the magnetic structure of Mn-spins is characterized by an ab -cycloid that accurately describes the direction of the observed ferroelectric polarization via the DM interaction. Our finding validates the model that the polarization flops found in the perovskite manganites result from the flop of the Mn-spin cycloid.

The manganite TbMnO₃ crystallizes in the orthorhombic perovskites structure $Pbnm$. On cooling, below $T_N=41\text{K}$ Mn spins order incommensurately point along the magnetic wave vector $\tau \sim 0.275\mathbf{b}^*$ [5, 6]. On further cooling below $T_S=28\text{K}$, a c -axis component of the Mn moment orders with a phase shift of $\pi/2$ with respect to the b -component so as to form a cycloidal structure where

Mn-spins rotate within the bc plane and around the a -axis as shown in Fig. 1(a) [5]. The axis of spin rotation defines the DM interaction, $\mathbf{S}_i \times \mathbf{S}_{i+1}$, while the distance $\mathbf{r}_{i,i+1}$ is parallel to the modulation vector τ . For this type of spin order, inversion symmetry is broken yielding for $R=\text{Tb and Dy}$, a ferroelectric polarization along the c -axis as indeed is observed ($\mathbf{P}_s||\mathbf{c} \sim \mathbf{a} \times \mathbf{b}$) [5, 6].

It is tempting to assume that the flop in the ferroelectric polarization arises from a flop in the Mn-spin spiral, but so far there is no experimental prove for this. Furthermore, the field dependence of the Mn-spin spiral is difficult to analyse as single-ion anisotropy terms of Mn and R need to be taken into consideration as well as the R -Mn interaction. The fact that in this $P||a$ phase Mn-spins order commensurately with $\tau = \frac{1}{4}\mathbf{b}^*$ [15, 16] render the cycloidal flop model even more complex. For such a commensurate spin structure it has been proposed that spin frustration and super-exchange induce lattice distortions that break inversion symmetry thereby generating the observed direction of the polarization at high field [13, 14, 15]. This exchange striction model can be applied only to a commensurate order, ruling out its validity for $R=\text{Dy}$ [17]. The observation that infrared electromagnon signals are always polarized along the a -axis irrespective if \mathbf{P}_s is parallel to the a - or c -axis further adds to the debate of the high field magnetic phases in these manganites [18]. A cycloidal Mn magnetic ordering that yields $P||a$ in zero field has been observed for $\text{Gd}_{0.7}\text{Tb}_{0.3}\text{MnO}_3$ [19], however, there is no direct evidence that the magnetic field flops the Mn-cycloid to yield a $P||a$ polarization. It is therefore pressing to establish an accurate model of the high field magnetic structure of these multiferroic manganites.

TbMnO₃ single crystals were obtained by re-crystallizing a ceramic rod under Ar atmosphere using an optical floating-zone furnace. The field and temperature dependence of the magnetic propagation wave vector was measured on the E4 double axis neutron diffractometer at the BENSC facility of the Helmholtz Zentrum Berlin

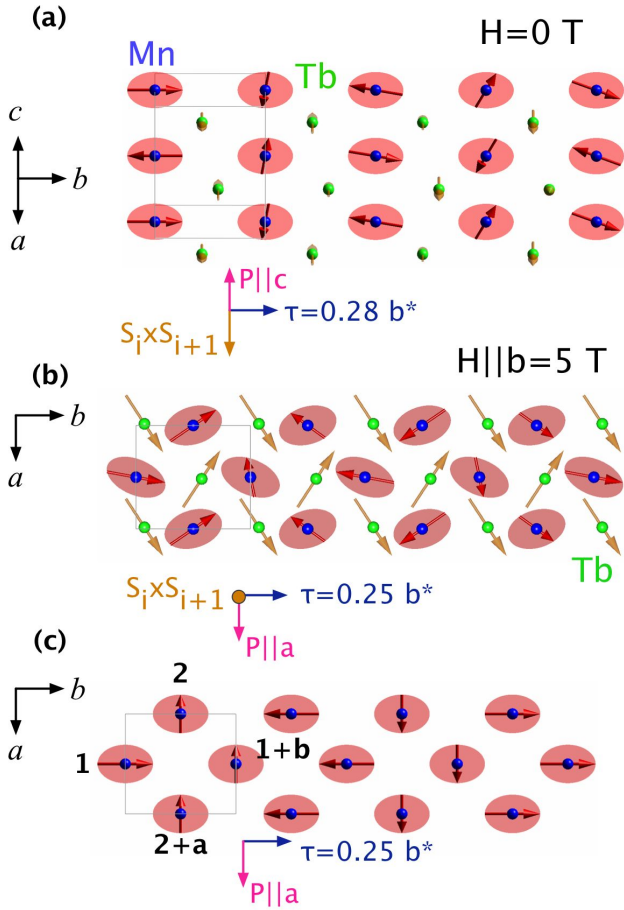


FIG. 1: (Color online) (a,b) Illustrations of the two cycloidal Mn magnetic structures proposed to cause ferroelectricity in TbMnO₃. In both cases the magnetic propagation vector τ is parallel to the b -axis. In zero field (panel (a)) cycloidal order, Mn spins rotate around the a -axis ($S_i \times S_{i+1}$) and rotate wholly within the bc -plane. The ferroelectric polarization via the antisymmetric DM interaction is produced along the c -axis. The high-field magnetic structure determined in this work is shown in panel (b), it yields a $P||a$ ferroelectric polarization that arises from an ab cycloid where Mn spins rotate around the c -axis. In both panels we also show the magnetic ordering of Tb-spins. In the zero field case (a), the magnetic propagation vectors of Tb and Mn-spins are clamped and Tb-spins point along the a -axis forming a SDW [5]. The canted antiferromagnetic ordering of Tb-spins for $H||b=5T$ determined in this work is shown in panel (b). (c) Here we depict an anharmonic ab -spiral where the phase difference between spins 1 and 2 is $\omega = \pi/2$. In such a case the angle between spins 1 and 2 is different from that between 2 and $1+b$ yielding an alternating scalar product along the b -axis. Amplitudes of Tb and Mn spins are not to scale.

using a neutron wave length of $\lambda=2.45\text{\AA}$ and a $\lambda/2$ filter placed in the incident beam. Here magnetic field was applied horizontally along the b -axis using the HM1 superconducting cryo-magnet. Due to the limited view of the sample in this magnet, integrated intensities of Bragg

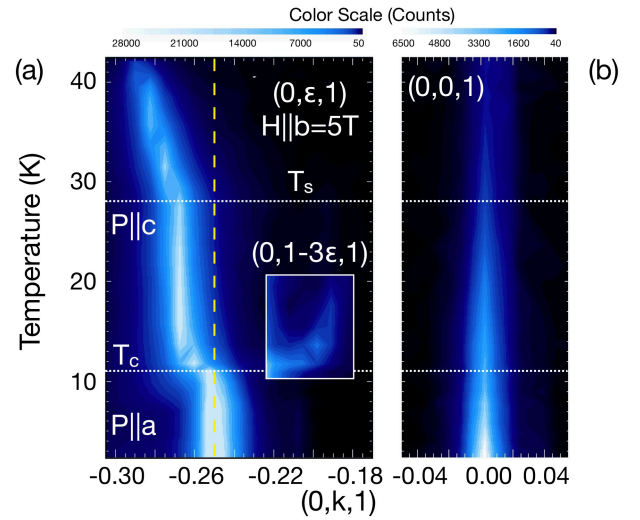


FIG. 2: (Color online) Single crystal neutron diffraction measurements from the E4 diffractometer. Here we show scans along $(0, k, 1)$ in reciprocal space as a function of temperature measured in a 5T field applied along the b -axis. The intensity of these scans is plotted in color coding with corresponding scales above each panel. (a) Portion of the data showing the temperature dependence of the A-mode reflection $(0, \epsilon, 1)$. Here the wave number ϵ varies from 0.282 at T_N to 0.266 at 15 K before it locks discontinuously to the commensurate value of $\frac{1}{4}$ below 11K. The weak third harmonic reflection was also observed in these scans to disappear at this transition. These data are shown in an enhanced color scale on the same panel and in the same location in the $T - Q$ map. (b) Temperature evolution of the $Pbnm$ forbidden reflection $(0,0,1)$.

reflections could only be measured within certain regions of the $0kl$ lattice plane, a situation that prohibits accurate analysis of the magnetic structure. To overcome this problem we conducted measurements using the D23 neutron single-crystal diffractometer installed at the Institut Laue-Langevin (ILL) with $\lambda = 1.281\text{\AA}$, that is equipped with a lifting detector that allows measurements of Bragg reflections above and below the scattering plane. Magnetic field was applied using the 6T vertical field superconducting magnet with an asymmetric vertical opening angle of $-5/+10^\circ$. For these measurements a single crystal of TbMnO₃ was cut into a parallelepiped with dimension $3.0 \times 2.9 \times 3.7\text{mm}$ with each face perpendicular to one crystallographic direction. The crystal was oriented with the b -axis parallel to the field. This geometry allowed us to measure reflections with k from -1.8 to 0.25 . In total 138 independent nuclear Bragg reflections consisting of 310 individual reflections were collected at $H = 0T$ and $T=8.5K$ within a range of $(0.07 \leq \sin(\theta)/\lambda \leq 0.69)$. At 8.5K the magnetic field was applied along the b -axis to 5T. In these conditions 140 commensurate ($\tau = 0$) independent Bragg reflections consisting of 160 individual reflections were measured along with 64 independent reflections with $\tau = \frac{1}{4}b^*$. Analytical absorption correc-

tions for each reflection were made by the Xtal suite of program, while analysis of the magnetic intensities was performed with the Fullprof code.

In Fig. 2(a) we show measurements of the $(0, \epsilon, 1)$ reflection as a function of temperature with $H \parallel b = 5\text{T}$ measured on the E4 diffractometer. The data shows that Mn-spin ordering is first observed at $T_N = 41\text{K}$ with the wave number ϵ decreasing on cooling. At $T_c = 11\text{K}$, ϵ changes discontinuously to yield a commensurate wave vector of $\tau = \frac{1}{4}\mathbf{b}^*$ [15, 16, 20]. Published polarization data shows that a $P \parallel c$ state develops below T_S while the polarization flops to $P \parallel a$ at T_c , coinciding with the transition to the commensurate magnetic phase [21]. In the same data we observe that the third harmonic reflection $(0, 1 - 3\epsilon, 1)$ rapidly changes its position and disappears also at T_c (Fig. 2(a)). On cooling below T_N we find an enhancement in the intensity of several nuclear reflections and the appearance of forbidden reflections such as the $(0, 0, 1)$ shown in Fig. 2(b). As we discuss below these effects arise from the ordering of Tb-spins with magnetic propagation vector $\tau^{Tb} = 0$.

To determine the magnetic structure of TbMnO_3 in the $P \parallel a$ state we utilized the D23 diffractometer. Here the sample was cooled in zero field to 8.5K and then a $H \parallel b = 5\text{T}$ was applied so as to enter the commensurate $P \parallel a$ phase that was confirmed by measurements of the magnetic vector. At this field and temperature we find that the most intense magnetic reflections with wave number $\epsilon = \frac{1}{4}$, have extinction condition $h + k = \text{even}, l = \text{odd}$ (A-mode) [24], while reflections with $h + k = \text{odd}, l = \text{odd}$ (G-mode) were considerably weaker. For space group $Pbnm$ and wave vector $\tau \leq \frac{1}{4}\mathbf{b}^*$ there are four irreducible representations (irreps) Γ of the magnetic symmetry for the Mn-ion [22, 23]. The A mode reflections are contained only in irreps Γ_1, Γ_2 and Γ_3 . Analysis of the data using only A-mode reflections and a single irrep did not result in a satisfactory fit to the data. This led us to consider combinations of representations. Of the possible combinations only a model using $\Gamma_1 \otimes \Gamma_3$ produced a satisfactory result with $R(F^2) = 7.9\%$ and $R_w(F^2) = 8.5\%$. This coupled irrep has the form of $(A_x, G_y, C_z) \otimes (G_x, A_y, F_z)$. Our measurements showed that F- and C- modes were at the very limit of detection indicating that the Mn moment is essentially contained within the ab -plane. Reflections from these modes were not included in the final refinements. [25] Our analysis yielded a magnetic structure for Mn given by the moment in μ_B : $m^{Mn} = \Gamma_1(2.83(12), 0.51(4), 0) \otimes \Gamma_3(0.55(4), 3.79(7), 0)$. The phase between the two irreps is also a variable parameter found to be $0.474(12)\pi$ close to $\frac{\pi}{2}$ expected for a cycloid. [26] The values of the Mn-spins in this commensurate cycloidal structure along the a - and b -axis are given in Fig. 3 for the $z=0$ and $z = \frac{1}{2}$ layers.

The magnetic structure indicated by this model is dominated by the A modes of these two irreps (A_x and

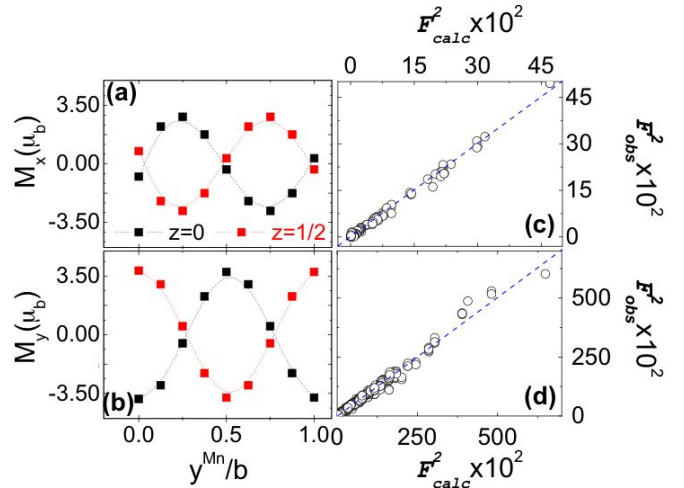


FIG. 3: (Color online) Results of refinements of the magnetic structure at 8.5K and $H \parallel b = 5\text{T}$. In panels (a) and (b) we show the variation of the M_x and M_y components of the Mn-spins for the ions located at $z=0$ (black) and $z = \frac{1}{2}$ (red) along the magnetic propagation vector. Note that the components along a and b are out of phase so as to yield a cycloidal ordering shown in Fig. 1. In panels (c) and (d) we show the comparison between observed and calculated magnetic structure factors (F^2) for the analysis of the Mn $\tau = \frac{1}{4}$ reflections and nuclear plus Tb-magnetic reflections respectively. Since the Tb magnetic propagation vector is $\tau = 0$ the nuclear and magnetic reflections are not separated in reciprocal space as in the case for the Mn-ions.

A_y) producing an elliptical cycloid, shown in Fig. 1(b). Here the Mn cycloid is contained within the ab -plane and Mn-spins rotate around the c -axis, consistent with the direction of the ferroelectric polarization along the a -axis ($\mathbf{P} \sim \mathbf{b} \times \mathbf{c}$). The anisotropy of the Mn cycloid in both low field bc and high field ab configurations appears to be very similar. In both cases the A_y mode possesses the higher moment (3.9 and $3.79 \mu_B/\text{Mn}$ respectively) while the components orthogonal to this mode are smaller and of the same magnitude ($2.8 \mu_B/\text{Mn}$). This result shows that the flop of the cycloidal plane does not effect the anisotropy of the Mn ordering itself. The deviation of the phase shift between the two irreps away from the ideal value produces an angle between spins of 85° . Despite this, $\mathbf{S}_i \times \mathbf{S}_{i+1}$ remains parallel to the c -axis and should not influence the magnitude of \mathbf{P}_s significantly. Finally for the Mn ordering we find that the G_x and G_y modes are active with amplitudes of $\sim 0.5 \mu_B/\text{Mn}$ and its net effect on the over all cycloidal order that produces a polarization along the a -axis is also relatively small.

We now turn our attention to the Tb-spin ordering. We find that in the $P \parallel a$ phase Tb-spins order commensurately with the underlying primitive lattice (i.e. $\tau^{Tb} = 0$). Analysis of the commensurate $Pbnm$ re-

flections clearly showed additional intensity that can be modelled by the Tb magnetic order. The best fit to the measured data was obtained for a ferromagnetic alignment of Tb-spins along the b -axis and antiferromagnetic coupling between nearest-neighbor Tb-spins along the $[110]$ direction (Fig. 1(b)). Analysis of this structure yields a total Tb moment of $7.24(7)\mu_B$, with an antiferromagnetic component of $6.07(9)\mu_B$ along the a -axis and a ferromagnetic component of $3.92(6)\mu_B$ along the b -axis. The ferromagnetic ordering along the b -axis is indeed evident in magnetization measurements under similar conditions[21].

The work we present here unambiguously proves that the commensurate $P||a$ phase in TbMnO_3 coincides with an ab Mn spin cycloid for $H||b=5\text{T}$. The antisymmetric DM interaction in this case does yield a ferroelectric polarization along the a -axis as indeed is observed ($\mathbf{P}_s||\mathbf{a} = \tau \times (\mathbf{S}_i \times \mathbf{S}_{i+1}) = \mathbf{c} \times \mathbf{b}$). We may thus identify the inverse DM interaction as the main mechanism for the magnetic-field induced flop of ferroelectric polarization.

In a perfect cycloidal magnetic arrangement the exchange mechanism proposed in references [13, 14] does not yield any ferroelectric polarisation, as the scalar product ($\mathbf{S}_i \cdot \mathbf{S}_{i+1}$) of neighboring spins is everywhere the same. This still holds for the commensurate perfectly circular spiral. In the case of an elliptical commensurate cycloid the exchange mechanism does cause ferroelectric polarization as the scalar product varies along the modulation. In our case with a modulation of four orthorhombic lattice distances the mechanism of [13, 14] may thus yield a finite polarisation along the a -direction which, however, should still be small due to the only minor deviation from a perfect circular cycloid. The exchange mechanism may gain further importance in the case of a very *anharmonic* cycloid. In the extreme anharmonic arrangement, where spins point either along the b or a directions yielding the sequence along the b -direction shown in fig. 1(c): left, up, right, down, there will be a very effective exchange striction mechanism as the scalar product $\mathbf{S}_i \cdot \mathbf{S}_{i+1}$, between nearest neighboring Mn ions alternates along the b -axis (in the example of fig. 1(c) the alternating angles are 90 and 0 deg. along the b -direction). In the current analysis we have performed, the phase difference between rows of cycloids propagating along the b -axis (e.g. in Fig. 1(c), rows starting at ions 1 and 2) is fixed by symmetry as $\omega = \pi\tau/2 = 45^\circ$ [23][27]. A deviation from this value will yield an anharmonic spiral, however such as case can not be fully tested with the current data and we can not exclude a small degree of anharmonicity. In view of the current debate about the electromagnon it appears interesting to add that this exchange-striction mechanism will always yield ferroelectric polarization along the a -direction.

In conclusion our work demonstrates that the flop in the ferroelectric polarization observed in TbMnO_3 arises

from the flop of the Mn cycloidal plane from bc to ab . The cycloidal magnetic structure we establish here for the high field $P||a$ phase does not possess a dominant ferroelectric mechanism based on exchange striction. The ordering of Tb-spins in this high field phase is that of a canted antiferromagnet giving a significant ferromagnetic component along the b -axis.

We acknowledge the assistance of L.C. Chapon and Juan Rodriguez-Carvajal with Fp-studio and Fullprof respectively. We thank M. Mostovoy and D. Khomskii for helpful discussions.

* Electronic address: argyriou@helmholtz-berlin.de

- [1] I. Dzyaloshinsky, J. Phys. Chem. Sol. **4**, 241 (1958).
- [2] T. Moriya, Phys. Rev. **120**, 91 (1960).
- [3] M. Mostovoy, Phys. Rev. Lett. **96**, 067601 (2006).
- [4] H. Katsura, N. Nagaosa, and A. V. Balatsky, Phys. Rev. Lett. **95**, 057205 (2005).
- [5] S.-W. Cheong and M. Mostovoy, Nat Mater **6**, 13 (2007).
- [6] T. Kimura, T. Goto, H. Shintani, K. Ishizaka, T. Arima, and Y. Tokura, Nature **426**, 55 (2003).
- [7] T. Goto, T. Kimura, G. Lawes, A. P. Ramirez, and Y. Tokura, Phys. Rev. Lett. **92**, 257201 (2004).
- [8] Y. Yamasaki, S. Miyasaka, Y. Kaneko, J. He, T. Arima, and Y. Tokura, Phys. Rev. Lett. **96**, 207204 (2006).
- [9] S. Park, Y. J. Choi, C. L. Zhang, and S.-W. Cheong, Phys. Rev. Lett. **98** (2007).
- [10] O. Heyer, N. Hollmann, I. Klassen, S. Jodlauk, L. Bohaty, P. Becker, J. A. Mydosh, T. Lorenz, and D. Khomskii, J. Phys. Cond. Matt. **18**, L471 (2006).
- [11] K. Taniguchi, N. Abe, T. Takenobu, Y. Iwasa, and T. Arima, Phys. Rev. Lett. **97**, 097203 (2006 Sep 1).
- [12] D. Senff, P. Link, N. Aliouane, D. N. Argyriou, and M. Braden, Phys. Rev. B **77**, 174419 (2008).
- [13] I. A. Sergienko and E. Dagotto, Phys. Rev. B **73**, 094434 (2006).
- [14] I. A. Sergienko, C. Sen, and E. Dagotto, Phys. Rev. Lett. **97**, 227204 (2006).
- [15] N. Aliouane, D. N. Argyriou, J. Stremper, I. Zegkinoglou, S. Landsgesell, and M. v. Zimmermann, Phys. Rev. B **73**, 020102 (2006).
- [16] T. Arima, T. Goto, Y. Yamasaki, S. Miyasaka, K. Ishii, M. Tsubota, T. Inami, Y. Murakami, and Y. Tokura, Phys. Rev. B **72**, 100102 (2005).
- [17] J. Stremper, B. Bohnenbuck, M. Mostovoy, N. Aliouane, D. N. Argyriou, F. Schrettle, J. Hemberger, A. Krimmel, and M. von Zimmermann, Phys. Rev. B **75**, 212402 (2007).
- [18] N. Kida, Y. Ikebe, Y. Takahashi, J. P. He, Y. Kaneko, Y. Yamasaki, R. Shimano, T. Arima, N. Nagaosa, and Y. Tokura, Phys. Rev. B **78**, 104414 (2008).
- [19] Y. Yamasaki, H. Sagayama, N. Abe, T. Arima, K. Sasai, M. Matsuura, K. Hirota, D. Okuyama, Y. Noda, and Y. Tokura, Phys. Rev. Lett. **101**, 097204 (2008).
- [20] D. Senff, P. Link, K. Hradil, A. Hiess, L. P. Regnault, Y. Sidis, N. Aliouane, D. N. Argyriou, and M. Braden, Phys. Rev. Lett. **98**, 137206 (2007).
- [21] T. Kimura, G. Lawes, T. Goto, Y. Tokura, and A. P. Ramirez, Phys. Rev. B **71**, 224425 (2005),

- [22] E. F. Bertaut, *Journal of Magnetism and Magnetic Materials* **24**, 267 (1981).
- [23] H. W. Brinks, J. Rodríguez-Carvajal, H. Fjellvåg, A. Kjekshus, and B. C. Hauback, *Phys. Rev. B* **63**, 094411 (2001).
- [24] h, k, l are Miller indices at the center of the primitive Brillouin zone
- [25] Reflections condition for the C-mode are $h + k = \text{even}$, $l = \text{even}$ and for the F-mode $h + k = \text{odd}$, $l = \text{even}$.
- [26] Our sensitivity to the phase difference was tested by fixing it to a value of $\pi/2$ which lead to statistically significantly higher R-factors of $R(F^2)=8.4\%$ and $R_w(F^2)=9\%$.
- [27] Here ω should not be confused with the phase difference between irreps Γ_1 and Γ_3 .